

Risk vessels of retropharyngeal hematoma during stellate ganglion block

Kazunori Hirota, MD¹, Kazuhiko Hirata, MD¹, Shiho Shibata, MD¹, Kenji Shigematsu, MD¹, Kazuo Higa, MD², Ken Yamaura, MD¹

5

¹Department of Anesthesiology, Fukuoka University School of Medicine, Fukuoka, Japan

²Care Center Himawarien, Fukuoka, Japan

This work was executed at Fukuoka University Hospital.

10

Running title: Risk vessels during stellate ganglion block

Corresponding author:

Ken Yamaura, MD

15

Department of Anesthesiology

Fukuoka University School of Medicine

7-45-1 Nanakuma, Jonan-ku,

Fukuoka 814-0180, Japan

Phone: +81-92-801-1011

20

Fax: +81-92-801-1025

E-mail: keny@fukuoka-u.ac.jp

This study was approved by Institutional review board (approval number 7-03 08-25)

25 Fukuoka University School of Medicine, Fukuoka, Japan

This work was not supported financially by any commercial source.

Abstract

30 **Background and Objective:** Bleeding into the retropharyngeal space is a potential complication in stellate ganglion block (SGB). Hematoma formation is considered to be due to damage of small arteries in the region, though only scanty details of the region are available. The aim of this study was to map the risk blood vessels in the retropharyngeal space to avoid accidental damage during SGB.

35 **Methods:** Contrast-enhanced three-dimensional computerized tomographic (3D-CT) images performed for 80 patients were re-analyzed retrospectively to construct detailed map of cervical blood vessels that are prone to damage and bleeding during SGB.

Results: Of the 160 bilateral necks, six (3.8%) and 82 (51.3%) small arteries were
40 identified in the medial portions of the ventral surface of the transverse processes of the 6th and 7th cervical vertebrae, respectively. In particular, 5 of the 6 small arteries detected in the medial portion of the ventral surface of the transverse process of the 6th cervical vertebra were the inferior thyroid artery (ITA). Of the 160 vertebral arteries, 2 arteries were missing, 4 (2.5%) entered the transverse foramen of the 5th cervical
45 vertebra, while one (0.6%) entered the transverse foramen of the 4th cervical vertebra.

Conclusions: 3D-CT identified the ITA in the medial portion of the ventral surface of the transverse process of the 6th cervical vertebra. The risk vessels of retropharyngeal hematoma during stellate ganglion block could include the ITA.

(229 words)

Introduction

Hematoma in the retropharyngeal space is a serious complication of stellate ganglion block (SGB), and which can be fatal due to airway narrowing and closure by compression of the trachea¹⁻⁴. Hematoma in the retropharyngeal space is thought to be
55 caused by damage of small arteries, rather than large vessels, such as the internal carotid artery and vertebral arteries⁵⁻⁶. However, identification of small vessels is often difficult, even by ultrasonography, due to the anatomical relation with the thyroid gland and the complex courses of the blood vessels⁷⁻⁸.

Three-dimensional computerized tomography (3D-CT) with a contrast medium
60 has recently been introduced. This imaging modality allows identification of obscure blood vessels in the head and neck region. The purpose of this study was to identify hematoma risk blood vessels present in the retropharyngeal space as assessed by 3D-CT.

65 **Methods**

In this study, we reviewed and re-analyzed retrospectively the contrast-enhanced 3D-CT records of adult patients who underwent angiographic examination of the head and neck region at three hospitals (Baba Hospital, Fukuoka University Chikushi Hospital, and Fukuoka University Hospital) between December 70 2007 and December 2009. The CT apparatus used in these hospitals were Toshiba Aquilion 64 (Toshiba Medical System Corporation; Ohtawara, Japan) and Siemens SOMATOM Sensation Cardiac 64 (Siemens Healthcare; Erlangen, Germany). The imaging conditions were set at 120 kV, 300 mA, 0.5-0.75 sec, with slice thickness of 0.5 mm. The contrast agent was 65-75 mL of iopamidol 300 or 370. Image analysis 75 was performed by radiologists using Ziostation (System 610; Ziosoft, Inc., Tokyo, Japan). The smallest blood vessels that could be identified were those with inner diameter of approximately 0.35-0.6 mm. Institutional Review Board approval for this retrospective study was obtained from Fukuoka University Hospital (IRB No. 7-03 08-25).

80 SGB is carried out using the transverse processes of the cervical vertebrae as guideposts. Accordingly, the 3D-CT images of the transverse processes were divided into different compartments for detailed examination of blood vessel distribution present in the vicinity of these processes (Figure 1). Specifically, the transverse processes of the 5th, 6th, and 7th cervical vertebrae were divided into medial and lateral 85 portions. For the 5th and 6th cervical vertebrae, the medial portion of each transverse process represented the area from the origin of the transverse process to the tip of the anterior tubercle, while the lateral portion represented the area from the tip of the

anterior tubercle to the tip of the posterior tubercle. For the 7th cervical vertebra, the anterior tubercle of the transverse process was not clear, and accordingly we divided
90 the area from the origin of the transverse process to its tip into two halves; the medial and lateral portions. Thus, the three vertebral bodies were divided into 12 regions bilaterally. A single radiologist subjected the 3D-CT images of the neck to computer processing and manually excluded the thyroid and carotid arteries to clarify the relationships between the cervical vertebrae and the cervical arteries. The
95 retropharyngeal space is located between the buccopharyngeal fascia on the dorsal side of the esophagus and the anterior lobe of the cervical fascia on the ventral side of the vertebral body. Next, the small arteries of interest represented those on the dorsal side of the trachea and the ventral side of the transverse process, while those on the ventral side of the posterior wall of the trachea were excluded. The carotid and
100 vertebral arteries were also excluded from the small arteries of interest.

Results

The 3D-CTs of 80 patients (55 men, 25 women, age 71.2 ± 9.0 years, mean \pm SD) were examined. Small arteries were identified on the ventral surfaces of the transverse processes of the 5th and 6th cervical vertebrae in 19 and 39 patients. There were 38 small arteries, (18 (22.5%) on the right side and 20 (25.0%) on the left side) on the ventral surface of the transverse process of the 6th cervical vertebra. Furthermore in the medial portion of the ventral surface of the transverse process of the 6th cervical vertebra, there were 6 (3.8%) small arteries in total, one (1.3%) on the right side and 5 (6.3%) on the left side. Many small arteries were identified on the medial portion of the ventral surface of the transverse process of the 7th cervical vertebra (82, 51.3% in total), including 43 (53.8%) on the right side and 39 (48.8%) on the left side, which were more than that of the 6th cervical vertebra (Table 1).

Based on anatomical positional relationship, five of the six small arteries detected in the medial portion of the ventral surface of the transverse process of the 6th cervical vertebra were the inferior thyroid arteries (ITA). These arteries passed on the cranial side of the normal position (Figure 2). The average diameter of all ITA was 1.26 ± 0.21 mm according to analysis of 3D-CT images. The remaining small artery could not be clearly identified due to a malformation.

The vertebral artery was missing in 2 patients (2 arteries) of the 80 patients. In 78 patients, 4 of 158 vertebral arteries entered the transverse foramen of the 5th cervical vertebra, 3 on the right side and one on the left side. One vertebral artery entered the transverse foramen of the 4th cervical vertebrae on right side. The rest 153 vertebral arteries entered the transverse foramen of the 6th cervical vertebra on both

125 sides.

Discussion

SGB is performed at the anterior tubercle of the transverse process of the 6th or 7th cervical vertebra. Accordingly, damage of small arteries located at the ventral surface of the transverse processes of these vertebrae with subsequent bleeding can potentially occur. During SGB through the anterior approach, blood vessels found by ultrasonography at the level of the 6th and 7th cervical vertebrae are at risk of bleeding by the puncture needle, but identification of the small arteries is often difficult⁸. Since the small arteries in this region show considerable variation in branching from the subclavian artery⁹⁻¹⁰, their courses show great individual differences, and they can be obscured by the thyroid gland. The present study eliminated the thyroid and carotid arteries by digital image processing of the contrast-enhanced 3D-CT images. This allowed visualization of the small arteries and elucidation of the courses of the arteries on the ventral surface of the transverse processes of the lower cervical vertebrae¹¹.

Siegenthaler⁸ employed ultrasonography and identified small arteries on the right side in 20% of the patients and on the left side in 28.3% of the patients, on the ventral surface of the transverse process of the 6th cervical vertebra, and, in 16.7% and 20.0% of the patients on the 7th cervical vertebra respectively. The present data show a smaller percentage of small arteries in close proximity of the 6th cervical vertebra and a higher percentage on the 7th cervical vertebra. This discrepancy can be attributed to difference in the examination methods. 3D-CT imaging allows the identification of the level of cervical vertebra. In the present study, a contrast medium was used in 3D-CT imaging, which made it easier and more accurate to detect small vessels.

The small arteries on the ventral surface of the transverse processes were ITA,

150 ascending cervical artery and transverse cervical artery which branches from the
subclavian artery. Furthermore, five of six small arteries seen on the medial side of the
ventral surface of the transverse process of the 6th cervical vertebra were identified
ITA. The ITA has an internal diameter of about 1.5 mm and branches from the
thyrocervical artery, which branches from the subclavian artery^{12, 13}. In this present
155 study, its diameter was 1.26 ± 0.21 mm according to analysis of 3D-CT images. It
ascends, then courses medially and inferiorly in the vicinity of the medial portion of
the ventral surface of the 7th cervical vertebra on the dorsal side of the common
carotid artery, and it finally enters the inferior lobe of the thyroid gland posteriorly.
The artery then travels medially and inferiorly, and enters the inferior lobe of the
160 thyroid dorsally. In most cases, at its highest point, the ascending ITA does not reach
over the 6th cervical vertebra.

Achievement of SGB through the inner side of the transverse process of the 6th
cervical vertebra is considered to be rarely associated with accidental puncture of the
ITA¹⁴. However, the present study showed that the left ITA passes on the rostral side
165 of the transverse process of the 7th cervical vertebra and some of them reaches the
medial portion of the ventral surface of the transverse process of the 6th cervical
vertebra, which can be damaged by puncture needle even when SGB is performed at
the level of the 6th cervical vertebra. The process of separation the tissues with the
fingertips during insertion of the needle can result in lateral displacement of the small
170 arteries in the anterior neck, in addition to displacement of the common carotid artery,
or their medial displacement along with the thyroid. Accordingly, we speculate that
such maneuver can potentially damage the ITA while it is being pulled from both sides

and its tension increased, with subsequent massive bleeding. Lateral approach with ultrasound guide may be better to avoid the risk of damaging inferior thyroid artery.

175 The vertebral artery typically enters the transverse foramen of the 6th cervical vertebra. However, in this study, 4/158 (2.5%) vertebral arteries entered the transverse foramen of the 5th cervical vertebra rather than the 6th cervical vertebra, which was slightly lower than the incidence of 8/120 (6.7%) reported by ultrasound imaging⁸. In addition, one vertebral artery entered the transverse foramen of the 4th cervical
180 vertebra, and there were 5 vertebral arteries that were exposed on the ventral side of the transverse process of the 6th cervical vertebra. To our knowledge, there are no reports of deaths caused by vertebral artery damage following performance of SGB, but attention should be taken to avoid bleeding due to erroneous puncture. For a safe SGB, to avoid vessel puncture we recommend utmost care by using ultrasound
185 guidance, consider approaches that are different from the conventional approach, and avoid placing strain on the ITA¹⁵.

 The present study has several limitations. First, it was retrospective in design, stressing the need to confirm the results in a prospective study. Second, the sample size was small to give a true results. Third, a single and independent radiologist
190 analyzed the 3D-CT images, but in order to ensure reproducibility of the findings two independent assessors should have done it. Fourth, we supposed the respiratory obstruction in retropharyngeal hematoma is caused by mechanical compression of the rigid trachea due to damage of small arteries in this study. However, it could be state of obstruction by swelling of the pharyngolarynx due to venous and lymphatic
195 congestion^{5, 16}, and we could not address it in this study. Fifth, the study patients had

head and neck disorders and one cannot rule out anatomical abnormalities, including the topographic distribution of brain and neck blood vessels, compared with healthy individuals.

200

In conclusion, the number of small arteries in the medial portion of the ventral side of the transverse process of the cervical vertebra was smaller in the 6th cervical vertebra than the 7th cervical vertebra. The ITA could be easily injured during SGB, resulting in hematoma formation in the retropharyngeal space. This finding suggests that the risk of damage to blood vessels during the process of SGB may be lower using the approach of the 6th cervical vertebra. However, utmost care should be exercised even when SGB is performed through the medial portion of the 6th cervical vertebra to avoid injury of small arteries, such as the ITA.

205

210 **Acknowledgments**

The authors are grateful to all the radiologists of Baba Hospital, Fukuoka University Chikushi Hospital and Fukuoka University Hospital for their invaluable cooperation with image analysis. The authors also thank F. G. Issa, MD, PhD (www.word-medex.com.au) for careful reading and editing of the manuscript.

215

References

1. Okuda Y, Urabe K, Kitajima T: Retropharyngeal or cervicomediastinal haematomas following stellate ganglion block. *Eur J Anaesthesiol* 2003; 20: 757-759
- 220 2. Mishio M, Matsumoto T, Okuda Y, et al: Delayed severe airway obstruction due to hematoma following stellate ganglion block. *Reg Anesth Pain Med* 1998; 23: 516-519
3. Takanami I, Abiko T, Koizumi S: Life-threatening airway obstruction due to retropharyngeal and cervicomediastinal hematomas following stellate ganglion
225 block. *Thorac Cardiovasc Surg* 2009; 57: 311-312
4. Kashiwagi M, Ikeda N, Tsuji A, Kudo K: Sudden unexpected death following stellate ganglion block. *Leg Med* 1999; 1: 262-265
5. Higa K, Hirata K, Hirota K, et al: Retropharyngeal hematoma after stellate ganglion block. Analysis of 27 patients reported in the literature.
230 *Anesthesiology* 2006; 105: 1238-1245
6. Huntoon MA: The vertebral artery is unlikely to be the sole source of vascular complications occurring during stellate ganglion block. *Pain Pract* 2010; 10: 25-30
7. Bhatia A: Evaluation of sonoanatomy relevant to performing stellate ganglion blocks using anterior and lateral simulated approaches: an observational study.
235 *Can J Anesth* 2012; 59: 1040-1047
8. Siegenthaler A: Ultrasound imaging to estimate risk of esophageal and vascular puncture after conventional stellate ganglion block. *Reg Anesth Pain Med* 2012; 37: 224-227

9. Kaneko U: Nippon Human Anatomy. Nineteenth Edition. Tokyo Nanzando. 2000;
240 p67-68
10. Toni R: A meta-analysis of inferior thyroid artery variations in different human ethnic groups and their clinical implications. *Ann Anat* 2005; 187: 371-385
11. Kuszyk BS: CT angiography with volume rendering: imaging findings. *AJR* 1995; 165: 445-448
- 245 12. Huntoon MA: Anatomy of cervical intervertebral foramina: vulnerable arteries and ischemic neurologic injuries after transforaminal epidural injections, *Pain* 2005; 117: 104-111
13. Narouze SN, Provenzano DA: Sonographically guided cervical facet nerve and joint injections, *J Ultrasound Med* 2013; 32: 1885-1896
- 250 14. Narouze S: Beware of the "serpentine" inferior thyroid artery while performing stellate ganglion block. *Anesth Analg* 2009; 109: 289-90
15. Narouze S: Ultrasound-guided stellate ganglion block: safety and efficacy. *Curr Pain Headache Rep* 2014; 18: 424 DOI 10.1007/s11916-014-0424-5
- 255 16. Wells DG, Zelcer J, Wells GR, et al: A theoretical mechanism for massive supraglottic swelling following carotid endarterectomy.
Aust NZJ Surg 1988; 58: 979-981

Legends for figures

Figure 1. (a) Schematic diagrams of the ventral surface of the 5th and 6th cervical vertebrae. The medial portion represented the area from the origin of the transverse process to the tip of the anterior tubercle. The lateral portion represented the area from the tip of the anterior tubercle to the tip of the posterior tubercle. (b) Schematic diagram of the ventral surface of the 7th cervical vertebra. The area between the origin and tip of the transverse process was divided into the medial and lateral portions.

Figure 2. Typical 3D-CT of neck vessels in a representative patient. Note that the left inferior thyroid artery at the ventral side of the 6th cervical vertebra transverse process passes on the cranial side of the normal position.

Table 1. Number and percentage (%) of small arteries identified in each region

	Right side (n=80)		Left side (n=80)	
	Medial (%)	Lateral (%)	Medial (%)	Lateral (%)
C5	0	10 (12.5)	0	9 (11.3)
C6	1 (1.3)	17 (21.3)	5 (6.3)	16 (20.0)
C7	43 (53.8)	38 (47.5)	39 (48.8)	38 (47.5)
Total	44	65	44	63

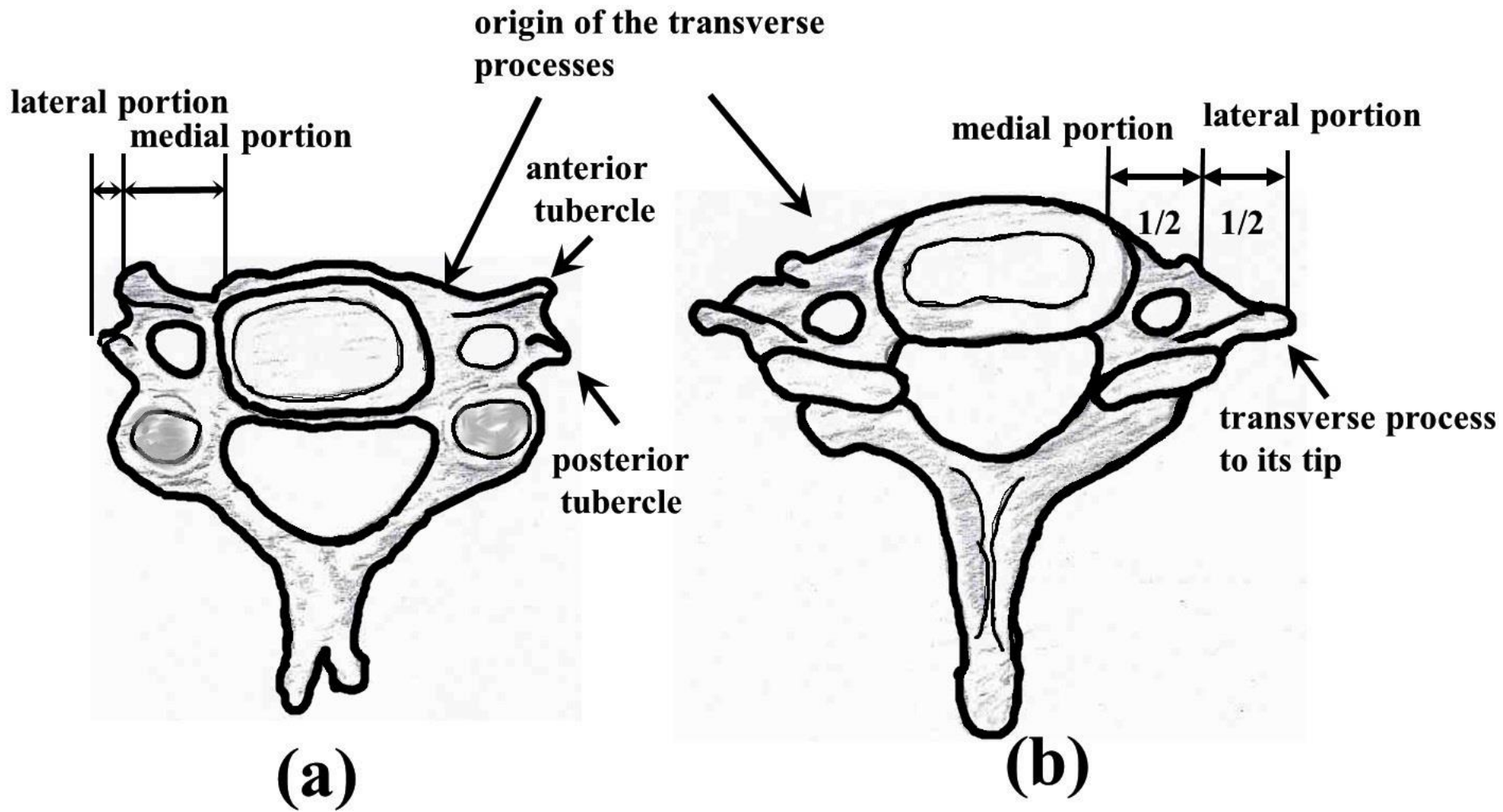


Fig. 1

right inferior
thyroid artery

left inferior
thyroid artery

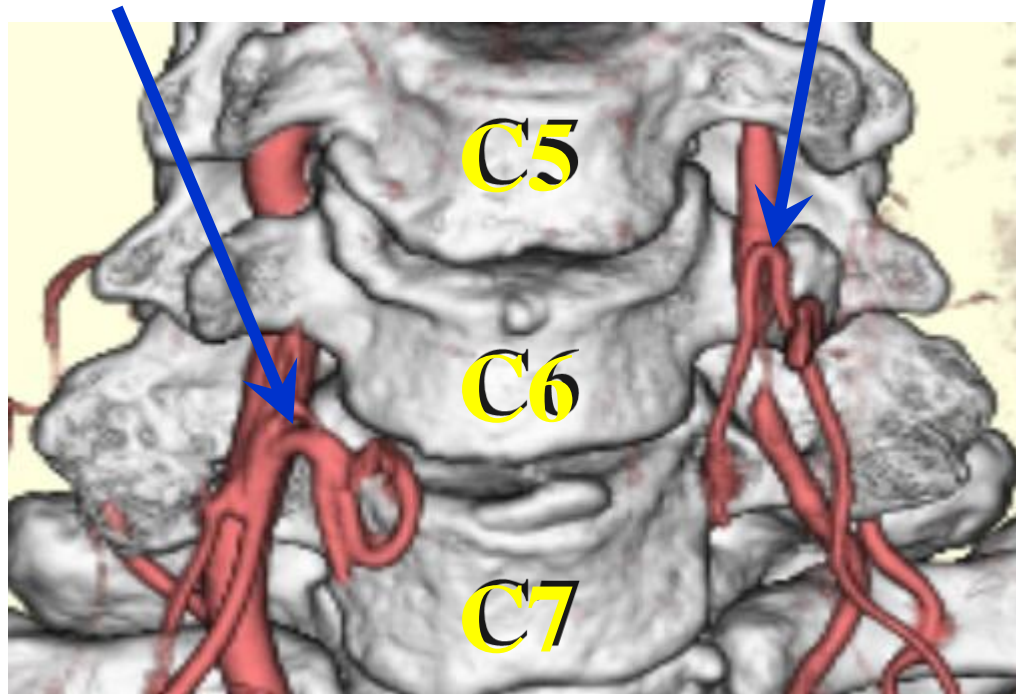


Fig. 2.